

The Effect of Thermal Contact Conductance (TCC) Between Aggregate Inclusion and Matrix on Thermal Conductivity of Cement-Based Material

Sokvisal Mom^{1,2*}, Sela Hoeun¹, Fabrice Bernard¹, Siham Kamali-Bernard¹, Virak Han²

¹Laboratory of Civil Engineering and Mechanical Engineering (LGCGM), INSA Rennes, 20 Avenue des Buttes de Coësmes, Rennes, 35700, FRANCE

²Institute of Technology of Cambodia
Russian Federation Blvd., P.O. Box 86, Phnom Penh, CAMBODIA

*Corresponding Author

DOI: <https://doi.org/10.30880/ijie.2022.14.05.011>

Received 25 April 2022; Accepted 15 July 2022; Available online 25 August 2022

Abstract: The effect of Thermal Contact Conductance (TCC) on thermal conductivity of mortar has been studied at the interface between the limestone and cement paste. A novel methodology, which involves the use of Scanning Electron Microscope (SEM) to scan the image of the interface in mortar, the software PlotDigitizer to create a set of points of the interface, and the FE software Abaqus/CAE to perform heat transfer simulation, is proposed in this study. Moreover, several hypotheses at the interface such as the gaps, flaws, and Interfacial Transition Zone (ITZ) are also highlighted. Temperature drop, thermal conductivity, and the TCC coefficient has been calculated for each model in order to understand the effect of TCC on cement-based materials thermal properties. The results show that the temperature drops at the interface are very low and the TCC coefficients are very high so that it can be ignored in heat transfer simulation except for a large air gap at the interface. Thus, it can be concluded that the TCC has no influence on the thermal conductivity of mortar.

Keywords: The effect of thermal contact conductance, thermal conductivity, temperature drop, cement-based materials, heat transfer

1. Introduction

In the classic version of particles movement in thermodynamic, heat is the disorder form of kinetic energy that can be typically transferred from one source (hot) to another (cold) [1]. In solids, heat energy can be conducted by electrical carriers, lattice waves, electromagnetic waves, spin waves, or other excitations [2]. Moreover, for composite materials, temperature drop at the joint between two solids could lead to an important temperature difference. Thus, extensive knowledge of temperature drop at the joint is required [3]. In addition, several parameters are needed to be identified such as force at joint, surface roughness and slopes, material hardness and conductivity, contact spot, and temperature [4]–[6]. This phenomenon is called Thermal Contact Conductance (TCC) or reciprocally, Thermal Contact Resistance (TCR). To understand more about TCC, researchers have developed several simplified models such as Simple Kinetic Theory Models [6], Interpolated Simple Kinetic Theory Models and Simplified Yovanovich Intergral Gap Conductance Model (Simplified YIGC) [4]. Moreover, experimental work has also been done in order to compare with the existing model but it was claimed that additional and more accurate experimental results are needed for a range of important contact parameters [6].

As regards, a cement-based material is simply a hydraulic binder [7] that is employed in several applications, particularly in construction. Furthermore, cement-based materials are cement paste, mortar, and concrete and they are heterogeneous materials. In order to take into account their heterogeneity, cement-based materials may be divided into four different scales [8]. Nano-scale which is the scale of elementary cells of hardened cement paste [9], Micro-scale which is the scale of hydrated cement paste, Sub-Meso-scale which is the scale of mortar [10], and Meso-scale which is scale of concrete [11], [12]. As far as it is concerned, in a multi-scale analysis, the result from smaller scale is directly used as the input data for larger scale [13].

The thermal behaviour of massive concrete structure such as hydraulic dams, mat foundations, hydroelectric power stations, nuclear power plants and more distinguishes its own structure from other concrete work [14]. Chemical reactions in those massive concrete structures generate heat that is not dissipated quickly enough and can be sometimes quite high. This heat creates significant restrained volume change that results in tensile stresses and strains, then it induces cracks in the structure [15]. Many measurements, techniques and specific guidelines are required for this type of structures in order to minimize cracking [14], [15]. In addition, knowledge on heat transfer simulation of massive concrete structure is also necessary in order to have better understanding about its thermal behaviour and any precautions are needed before placing the concrete.

Cement-based materials, like other materials, have important thermal properties such as thermal conductivity (k), specific heat (c), thermal diffusivity (h_2), thermal expansion (α) and density (ρ) [16]. As far as the heterogeneity of cement-based materials is concerned, their thermal properties strongly depend on the thermal properties of the compositions, especially aggregates [17]. In addition, the density of cement-based materials is an important indicator to predict their thermal properties; for concrete, for example [16]. For instance, thermal conductivity of hemp concrete has been studied and the result shows that the thermal conductivity of hemp concrete increases while its density increases [18].

The objective of this paper is to understand the effect of Thermal Contact Conductance (TCC) or Thermal Contact Resistance (TCR) on thermal conductivity of cement-based materials. Temperature drop could occur at the level of Sub-Meso-scale (Mortar) and Meso-scale (Concrete) where there is contact between aggregate and matrix. In this paper, numerical modelling with FE software Abaqus had been used to perform heat transfer simulation at Sub-Meso-scale (Mortar) and to find out if TCC (or TCR) has an effect on the thermal properties of the mortar.

2. Initial simulation- Influence of Thermal Contact Conductance (TCC)

Referring to the previous argument in the introduction part, TCC (or TCR) has been involved in many fields such as aircraft, semiconductors and electronic device [19]. As mentioned above, TCC could be estimated by several simplified models, but it is still challenging to estimate the correct value owing to the uncertainty of several parameters. Concerning about the simplified models, TCC has been divided into two types of heat transfer through the interface, solid-to-solid contact spots and conduction across the gap via intermediate fluid [20]. The formulas of TCC has been proposed as below:

$$h_j = h_c + h_g \tag{1}$$

where:

h_j = thermal contact conductance at the joint,

h_c = thermal contact conductance of solid contact,

h_g = thermal contact conductance across the gap via intermediate fluid.

In this initial simulation, only the effect of TCC on the whole mortar has been studied. Then, the effect of interface on TCC will be discussed in the next section. The simplified of mortar in form of cube composed of only 2 phases with 1 (Fig. 1) and 27 inclusions (Fig. 2) have been simulated with different values of TCC, starting from 10^6 to $10^{-2} \text{W/m}^2\cdot\text{K}$, are imposed at the interface of matrix/aggregates. The thermal properties of the two phases are shown in Table 1 and Table 2. In addition, the boundary conditions are temperature of 373.15K on one side and 298.15K on the opposite side of the cube with 298.15K as the initial temperature of the mortar.

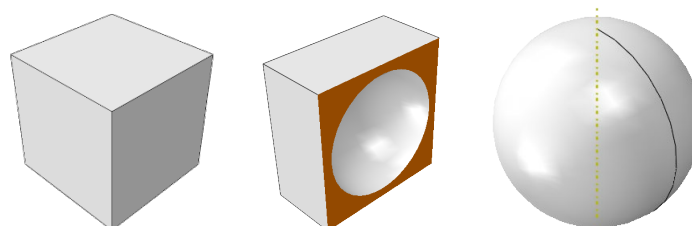


Fig. 1 - Simplified mortar with 1 inclusion

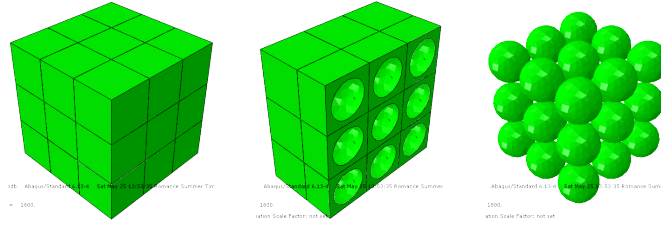


Fig. 2 - Simplified mortar with 27 inclusions

After the simulation, the value of heat flux come out from the lower temperature side of the mortar are retrieved and used to calculate the thermal conductivity (k). Then, the value of thermal conductivity is plotted as k/k_{max} in function of TCC (Fig. 3) whereas the k_{max} is the value of thermal conductivity without TCC. It is found out that the effect of TCC on thermal conductivity exists only when the value of TCC is equal or lower than $10^3 W/m^2.K$.

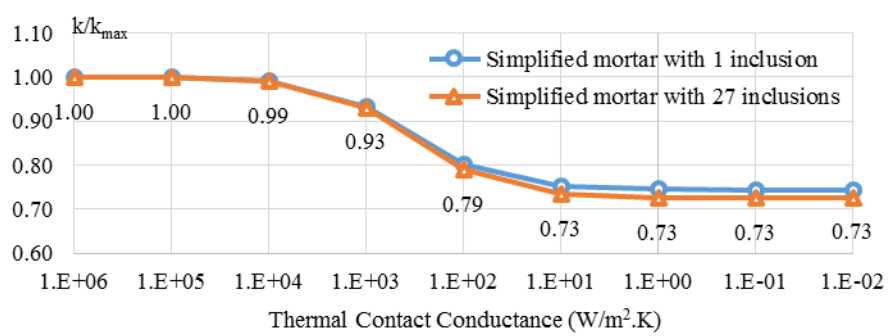


Fig. 3 - The effect of TCC on thermal conductivity of mortar

3. Materials Hypotheses and Simulation Methodology

In order to simplify the study of TCC, cement-based material at Sub-Meso-scale (mortar) has been chosen in this study. Like mentioned above, it is the scale at which the aggregates fraction appears to be important and the TCC could have influence at the interface matrix/aggregates. In this work, limestone (aggregate) and cement paste of CEM I 42.5R (matrix) with Water/Cement (W/C) ratio=0.4 are adopted. In addition, the cement pastes to aggregate ratio is 50%.

3.1 Materials Properties

Apart from limestone, sand, and cement paste, the other heterogeneities at the scale of mortar are ITZ, air and water porosity in the cement paste. Otherwise, due to the presence of ITZ, the original local porosity in cement paste has been modified and new porosity can be found by using Eq. (2).

$$\Phi_{matrix} = \Phi_{paste} \left(\frac{V_{matrix} + V_{ITZ}}{V_{matrix} + \alpha V_{ITZ}} \right) \quad (2)$$

where:

Φ_{matrix} = porosity of cement paste with the present of ITZ,

Φ_{paste} = porosity of cement paste without the present of ITZ,

V_{matrix} = Volume of cement paste,

V_{ITZ} = Volume of ITZ,

$\alpha = \Phi_{ITZ} / \Phi_{matrix}$ = Porosity ratio between ITZ and matrix, ranging from 1.5 to 2.

The thermal properties of the mortar's compositions are shown in Table 1 and the cement paste respected to its porosity in Table 2. Specific heat and thermal conductivity have been determined through a multi-scale modelling approach (not presented here).

Table 1 - Thermal properties of mortar’s composition

| | Density (kg/m ³) | Specific Heat (J/kg.K) | Thermal Conductivity (W/m.K) |
|------------------|---------------------------------|---------------------------|---------------------------------|
| Limestone | 2650 | 656 | 0.6 |
| Air | 1.208 | 1006 | 0.0262 |
| Water | 1000 | 4128 | 0.608 |

Table 2 - Thermal properties of cement paste with porosity

| | Porosity (%) | Density (kg/m ³) | Specific Heat (J/kg.K) | Thermal Conductivity (W/m.K) |
|---------------------|-----------------|---------------------------------|---------------------------|---------------------------------|
| Cement paste | 0.44 | 1707.371 | 1724 | 1.38 |
| | 0.31 | 1857.14 | 1341 | 1.39 |
| | 0.18 | 2018.166 | 1216 | 1.37 |

Moreover, in mortar, ITZ is more porous than the bulk cement paste and the porosity of bulk cement paste itself has also been modified from the original cement paste (before mixing with aggregate). For example, cement paste with porosity = 0.18 (Table 2) has transformed to ITZ with porosity = 0.247 and bulk cement paste with porosity = 0.123 (Table 3). Finally, the thermal properties of ITZ and bulk cement paste can be calculated by finding its corresponding porosity using Eq. (2) and interpolating the value of thermal properties from Table 2. In addition to the two tables above, Table 3 gives the thermal properties of ITZ and bulk cement paste with different porosities.

Table 3 - Thermal properties of ITZ and bulk cement paste

| | α | Porosity (%) | Density (kg/m ³) | Specific Heat (J/kg.K) | Thermal Conductivity (W/m.K) |
|------------------------------|----------|-----------------|---------------------------------|---------------------------|---------------------------------|
| ITZ | 1.5 | 0.22 | 1969.224 | 1253.992 | 1.376 |
| | 1.7 | 0.231 | 1954.415 | 1265.488 | 1.378 |
| | 1.85 | 0.239 | 1944.594 | 1273.112 | 1.379 |
| | 2 | 0.247 | 1935.702 | 1280.015 | 1.380 |
| Bulk cement paste | 1.5 | 0.146 | 2059.858 | 1183.636 | 1.365 |
| | 1.7 | 0.136 | 2072.472 | 1173.844 | 1.363 |
| | 1.85 | 0.129 | 2080.838 | 1167.349 | 1.362 |
| | 2 | 0.123 | 2088.413 | 1161.469 | 1.361 |

3.2 Geometries Construction, Hypothesis and Heat Transfer Simulation

First of all, the interface of matrix/aggregates is captured by SEM (Fig. 4(a)) and geometry model is only composed of two parts, limestone aggregate and cement paste (Fig. 4(b)). To precise, each part has 165µm long (330µm in total) with 330µm of thickness. Then, the image from SEM was uploaded to WebPlotDigitizer in order to extract the data (or coordinates) of the interface. Subsequently, the dataset was imported as sketch in Abaqus/CAE and, as the result, the interface profile is reconstructed by creating points from the dataset and connecting all the points using curve line (Fig. 5). For meshing, DC2D3 element is used at the interface and DC2D4 element for others. Finally, the surfaces between the two parts of the mortar are tied together. It means the temperature (or heat flux) is directly transfer to another surface without any temperature drops (or heat flux loss).

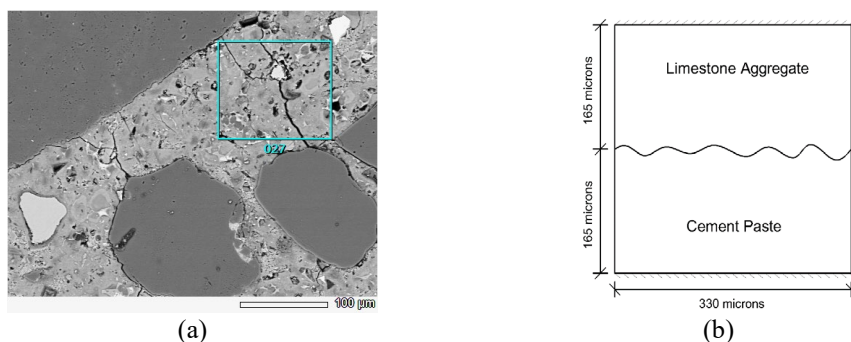


Fig. 4 - Interface of matrix/aggregates captured by SEM



Fig. 5 - Interface of matrix/aggregates regenerated in Abaqus/CAE

As far as it is concerned, boundary conditions for this simulations are temperatures of 373.15K at top, 298.15K at the bottom and 298.15K as initial temperature of the mortar (referring to the Fig. 4(b)). In addition, steady state heat transfer analysis is used, then thermal conductivity and gap conductance of mortar are calculated by Eq. (3) and Eq. (4) respectively.

$$k = \frac{Q \times L}{T_{hot} - T_{cold}} \tag{3}$$

where:

k = Thermal conductivity of mortar,

Q = Outgoing heat flux at where the temperature is equal to T_{cold} ,

L = Length of the mortar studied (330 μm),

T_{cold} , T_{hot} = Lower (298.15 K) and higher (373.15 K) boundary condition temperatures.

$$h_j = \left[\frac{T_{hot} - T_{cold}}{Q} - \frac{\Delta L_{lime\ stone}}{k_{lime\ stone}} - \frac{\Delta L_{cement\ paste}}{k_{cement\ paste}} \right]^{-1} \tag{4}$$

where:

ΔL_i = Length of each part of the sample (165 μm),

k_i = Thermal conductivity of the sample.

As regard, the interface of matrix/aggregates of the mortar, not only the interface profile is not perfect but also the bonding between the two surfaces where two things could occur, ITZ and flaw. In this study, the effect of ITZ and flaws (with different thickness and length) at the interface have been discussed. In addition to the flaw, two saturation ratios have also been compared, zero-saturation (air) and full-saturation (water).

To sum up, Table 4 summarizes all the hypotheses in this study including the smooth surface in the purpose of comparison.

Table 4 - Hypothesis for case study on TCC

| Interface type | Opening (μm) | Length (μm) | Fig. 6 |
|--|-------------------|-------------|--------|
| Non-rough | 0 | 0 | (a) |
| Rough | 0 | 0 | (b) |
| Air Gap | 3, 10, 20, 30, 40 | 330 | (c) |
| Water Gap | 3, 10, 20, 30, 40 | 330 | (c) |
| One air flaw | 3, 10, 20, 30, 40 | 100 | (d) |
| One water flaw | 3, 10, 20, 30, 40 | 100 | (d) |
| Two air flaws | 3, 10, 20, 30, 40 | 100 | (e) |
| Two water flaws | 3, 10, 20, 30, 40 | 100 | (e) |
| ITZ ($\alpha = 1.5, 1.7, 1.85, 2$) | 20, 40, 60 | 330 | (f) |

In relation to the simulation, Fig. 6 illustrates the interface matrix/aggregates of the mortar with different interfaces hypotheses. For instance, the non-rough (or smooth) (a) and rough surface (b), gap (c), one and two flaws (d and e), and ITZ (f) at the interface. By the way, in the case of one flaw, it is positioned in the middle of the surface and the defect ratio of this type of surface is around 30%. Moreover, for the two flaws, they are placed at the far end of the surface with the surface defect ratio equal to 67%. The distance between the two flaws is about 130μm.

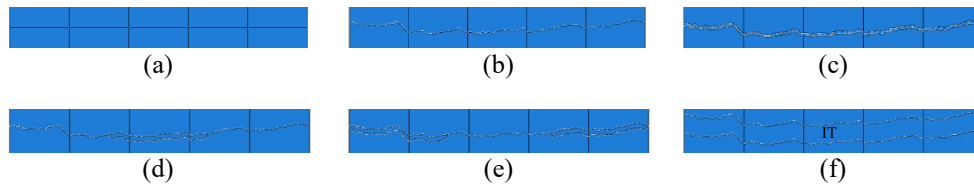


Fig. 6 - Interface of matrix/aggregates hypothesis in Abaqus

4. Results and Discussion

In this section, several parameters, such as temperature drop at interface, thermal conductivity and thermal contact conductance, have been discussed and compared for different hypotheses.

Concerning temperature drop, the temperature profiles of mortar are plotted. For the ease of comparison, the model has been equally divided into 12 average planes as shown in Fig. 7(a). Then, the average temperature is calculated for each plane and plotted in Fig. 7(b), and the plane number 6 and 7 are the interfaces between matrix and aggregates. In the first result, the interface with smooth and rough surfaces are compared and it is found out that the temperature drop for both types of surface is very low (0% for smooth and 0.016% for rough surface) to consider in the heat transfer simulation. Moreover, the thermal conductivity and TTC for mortar with smooth interface are 0.8W/m.K and $2.5 \times 10^9 \text{W/m}^2.\text{K}$ respectively. For mortar with rough interface, $k = 0.79 \text{W/m.K}$ and $h_j = 0.2 \times 10^9 \text{W/m}^2.\text{K}$. Additionally, all results for every types of interface are listed in Table 5.

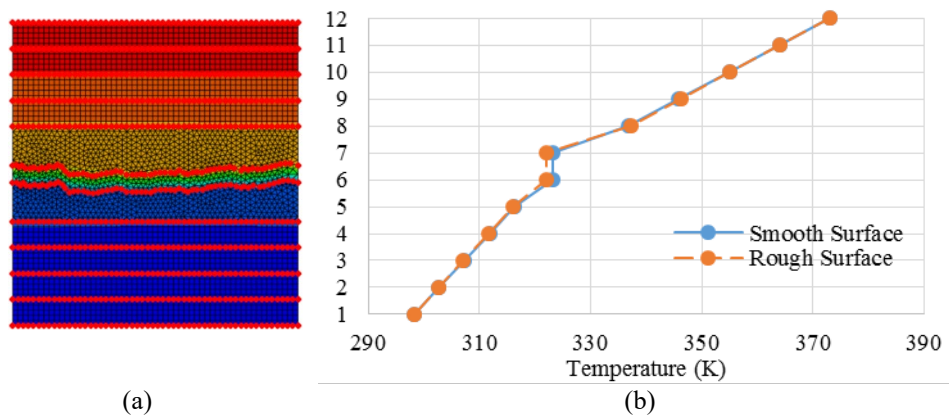


Fig. 7 - Temperature profile

As shown in Fig. 3, the influence of TCC on thermal conductivity starts from h_j smaller than $10^3 \text{W/m}^2.\text{K}$. Moreover, with the result from Table 5, it can be concluded that TCC has no influence on thermal conductivity at Sub-Meso-scale unless there is the air gap at the interface with a thickness larger than $30 \mu\text{m}$. In this case, the temperature drop at the interface is about 0.15%. Similarly, for ITZ, it does not have any influence on the thermal conductivity even with the largest fraction of porosity ($\alpha=2$) compared to the bulk cement paste. Thus, it is not necessary to consider of ITZ in heat transfer problem for cement-based materials, for example, mortar.

Table 5 - Temperature drop, thermal conductivity and TCC of mortar

| Interface type | Gap ($\mu\text{m} \times \mu\text{m}$) | Temperature drop (%) | k (W/m.K) | h_j (W/m ² .K) |
|---------------------|--|----------------------|-----------|-----------------------------|
| Non-rough | 0x0 | 0.00 | 0.80000 | 2424240000.06 |
| Rough | 0x0 | 0.016 | 0.79040 | 199654.90 |
| Air Gap | 3x330 | 0.05 | 0.63183 | 8730.52 |
| | 10x330 | 0.10 | 0.43618 | 2724.81 |
| | 20x330 | 0.13 | 0.30536 | 1362.95 |
| | 30x330 | 0.15 | 0.23497 | 893.16 |
| | 40x330 | 0.16 | 0.19363 | 667.40 |
| Water Gap | 3x330 | 0.00 | 0.78780 | 98066.66 |
| | 10x330 | 0.01 | 0.78279 | 45778.14 |
| | 20x330 | 0.02 | 0.77637 | 26098.77 |
| | 30x330 | 0.02 | 0.77040 | 18251.60 |
| One air flow | 3x100 | 0.01 | 0.76808 | 47514.83 |
| | 5x100 | 0.01 | 0.75126 | 37370.28 |

| | | | | |
|---|-------------|------|---------|-----------|
| | 10x100 | 0.02 | 0.75706 | 27317.05 |
| | 20x100 | 0.03 | 0.70516 | 18024.27 |
| | 30x100 | 0.03 | 0.73578 | 13025.06 |
| One water flow | 3x100 | 0.00 | 0.79593 | 170144.27 |
| | 5x100 | 0.00 | 0.78781 | 156631.13 |
| | 10x100 | 0.00 | 0.80915 | 130011.84 |
| | 20x100 | 0.01 | 0.78036 | 96332.96 |
| | 30x100 | 0.01 | 0.84514 | 74255.89 |
| Two air flows | 3x100 (x2) | 0.02 | 0.73499 | 24649.86 |
| | 5x100 (x2) | 0.03 | 0.69934 | 16843.46 |
| | 10x100 (x2) | 0.04 | 0.67178 | 10681.40 |
| | 20x100 (x2) | 0.06 | 0.56974 | 5998.33 |
| | 30x100 (x2) | 0.09 | 0.51515 | 3492.53 |
| Two water flows | 3x100 (x2) | 0.00 | 0.79460 | 152005.78 |
| | 5x100 (x2) | 0.00 | 0.78557 | 131949.82 |
| | 10x100 (x2) | 0.01 | 0.80425 | 97542.46 |
| | 20x100 (x2) | 0.01 | 0.77026 | 62786.51 |
| | 30x100 (x2) | 0.02 | 0.82668 | 43526.86 |
| ITZ ($\alpha = 1.5$) | | 0.01 | 0.82202 | 49450.13 |
| ITZ ($\alpha = 1.7$) | | 0.01 | 0.82176 | 49521.27 |
| ITZ ($\alpha = 1.85$) | 20x330 | 0.01 | 0.82163 | 49554.63 |
| ITZ ($\alpha = 2$) | | 0.01 | 0.82150 | 49588.26 |
| ITZ ($\alpha = 1.5$) | | 0.02 | 0.82223 | 28759.36 |
| ITZ ($\alpha = 1.7$) | | 0.02 | 0.82206 | 28799.48 |
| ITZ ($\alpha = 1.85$) | 40x330 | 0.02 | 0.82197 | 28821.48 |
| ITZ ($\alpha = 2$) | | 0.02 | 0.82188 | 28841.81 |
| ITZ ($\alpha = 1.5$) | | 0.03 | 0.82248 | 20283.60 |
| ITZ ($\alpha = 1.7$) | | 0.03 | 0.82240 | 20312.41 |
| ITZ ($\alpha = 1.85$) | 60x330 | 0.03 | 0.82235 | 20326.90 |
| ITZ ($\alpha = 2$) | | 0.03 | 0.82231 | 20341.44 |

5. Conclusion

At the Sub-Meso-scale (mortar), the presence of interfaces between matrix and aggregates (cement paste/limestone) characterized by a certain Thermal Contact Conductance (TCC) could influence thermal conductivity of the mortar. In addition to its effect on the mortar, several parameters have been discussed and it can be concluded that:

- The surfaces irregularities (asperities), flaws and gaps at the interface have no effect on thermal conductivity of mortar
- ITZ, even at high porosity volume fraction, has no effect on thermal conductivity of mortar
- The TCC has effect on thermal conductivity only when the air gap is larger than 30 μ m of thickness which can be obtained only in the case of the propagation of a macro-crack.

To sum up, when the heat transfer simulation is involved with the cement-based materials, especially at the mortar level, the inclusion's surface asperities, flaws, gaps, and ITZ can be ignored from the modelling. The model of the inclusion could be round spheres without any flaw or gap at the interface and the cement paste could be modelled as the original cement paste without ITZ.

References

- [1] Ilya P. & Dilip K. (1999). Thermodynamique. Des moteurs thermiques aux structures dissipatives. Odile Jacob.
- [2] Tritt T. M. (2004). Thermal conductivity: Theory, properties, and applications. Kluwer Academic/Plenum Publishers.
- [3] Salerno J. & Kittel P., (1997). A thermal contact conductance. NASA Technical Memorandum. Ames Research Center.
- [4] Song S., Yovanivich M. M. & Goodman F. O. (1993). Thermal gap conductance of conforming surfaces in contact. Journal of Heat Transfer, 115, 553–540.
- [5] Dou R., Ge T., Liu X. & Wen Z. (2016). Effects of contact pressure, interface temperature, and surface roughness on thermal contact conductance between stainless steel surfaces under atmosphere condition. International Journal of Heat and Mass Transfer, 94, 156–163.

- [6] Yovanivich M. M. (1982). Thermal contact correlations. Proceedings of the 16th Thermophysics Conference, Palo Alto, California, pp. 83–95
- [7] Abdel Rahman R. O. & Saleh H. E-D. (2018). Cement based materials. IntechOpen.
- [8] Bernard F., Fu J. & Kamali-Bernard S., (2018). Multiscale modeling approach to determine the specific heat of cementitious materials. *European Journal of Environmental and Civil Engineering*, 23(5), 535-551.
- [9] Fu J., Bernard F. & Kamali-Bernard S. (2017). First-principles calculations of typical anisotropic cubic and hexagonal structures and homogenized moduli estimation based on the Y-parameter: Application to CaO, MgO, CH and Calcite CaCO₃. *Journal of Physics and Chemistry of Solids*, 101, 74–89.
- [10] Bernard F. & Kamali-Bernard S., (2015). Numerical study of ITZ contribution on mechanical behavior and diffusivity of mortars. *Computational Materials Science*, 102, 250–257.
- [11] Kamali-Bernard S., Keinde D. and Bernard F. (2014). Effect of aggregate type on the concrete matrix/aggregates interface and its influence on the overall mechanical behavior. A numerical study. *KEM*, 617, 14–17.
- [12] Keinde D., Kamali-Bernard S., Bernard F. & Cisse I. (2014). Effect of the interfacial transition zone and the nature of the matrix-aggregate interface on the overall elastic and inelastic behaviour of concrete under compression: a 3D numerical study. *European Journal of Environmental and Civil Engineering*, 1167–1176.
- [13] Bernard F., Kamali-Bernard S. & Prince W. (2008). 3D multi-scale modelling of mechanical behaviour of sound and leached mortar. *Cement and Concrete Research*, 38, 449–58.
- [14] ACI 207.1R-05(R2012) (2012). Guide to mass concrete 2. American Concrete Institute.
- [15] Hasan N. (2020) Durability and sustainability of concrete: Case Studies for concrete exposures. Springer International Publishing.
- [16] Marshall A. L. (1972). The Thermal properties of concrete. *Building Science*, 7(3), 167–174.
- [17] Jin L., Zhang R. & Du X. (2017). Computational homogenization for thermal conduction in heterogeneous concrete after mechanical stress. *Construction and Building Materials*, 141, 222–234.
- [18] Collet F. and Pretot S. (2014). Thermal conductivity of hemp concretes: Variation with formulation, density and water content. *Construction and Building Materials*, 65, 612–619.
- [19] Pan X., Cui X., Liu S., Jiang Z., Wu Y. & Chen Z. (2020). Research progress of thermal contact resistance. *Journal of Low Temperature Physics*, 201, 213–253.
- [20] Madhusudana C. V. (2014). Thermal contact conductance. Springer International Publishing.